Open access • Journal Article • DOI:10.1038/319109A0

Future global warming from atmospheric trace gases — Source link

Robert E. Dickinson, Ralph J. Cicerone

Institutions: National Center for Atmospheric Research

Published on: 01 Dec 1986 - Nature (Nature Publishing Group)

Topics: Global warming and Trace gas

Future global warming from atmospheric trace gases

Robert E. Dickinson & Ralph J. Cicerone

National Center for Atmospheric Research, Boulder, Colorado 80307, USA

Human activity this century has increased the concentrations of atmospheric trace gases, which in turn has elevated global surface temperatures by blocking the escape of thermal infrared radiation. Natural climate variations are masking this temperature increase, but further additions of trace gases during the next 65 years could double or even quadruple the present effects, causing the global average temperature to rise by at least 1 °C and possibly by more than 5 °C. If the rise continues into the twenty-second century, the global average temperature may reach higher values than have occurred in the past 10 million years.

THE likelihood of global climate change from increasing concentrations of carbon dioxide is now well known[1-10]. Much more recent is the realization that other less-abundant trace gases are also increasing and that their change is likely in total to have an effect on climate comparable with that of carbon dioxide[11-21]. These include CH_4, tropospheric O_3, N_2O and the chlorofluorocarbons (CFCs) CCl_3F and CCl_2F_2. What do we know about the effect of these gases on climate, their temporal trends, and the implications of these increases? To see how such climate change can occur, we first consider the energy-exchange processes of the Earth-atmosphere system. The relative contribution of the various trace gases to climate change will be determined by their relative contributions to these energy processes.

Solar radiation is absorbed by the atmosphere and the Earth's surface, providing the energy required by many terrestrial processes. Figure 1 shows the amount of energy involved, on a global and annual average. For climate to be in equilibrium, this absorbed solar radiation must be balanced by outgoing thermal radiation. The partial trapping of this thermal radiation by radiatively-absorbing particles or molecules helps to increase surface temperatures by several tens of degrees compared with what they would be without the atmosphere. This process, sometimes called the 'greenhouse effect', occurs largely in the first 10–15 km of the atmosphere, that is, the troposphere. Radiatively active constituents both absorb and emit thermal radiation, depending on their effective cross-sections and on temperature. Their emission varies with the local atmospheric temperature, whereas their absorption depends on the temperatures of the other atmospheric layers and of the Earth's surface where the radiation was initially emitted. Because tropospheric temperatures decrease with increasing altitude, typically by 5–7 °C km^{-1}, the active atmospheric constituents absorb more upward radiative flux than they emit. Clouds and water vapour are the dominant contributors to this process.

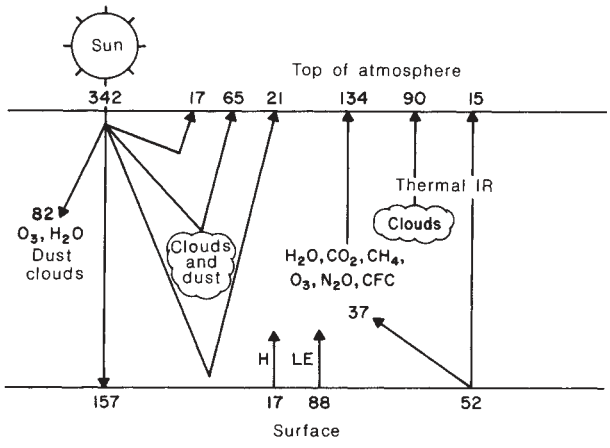

Fig. 1 Schematic depiction of the global and annual average fluxes of radiation within the climate system. Incident solar radiation is either absorbed or reflected as indicated on the left side. Most of the reflection occurs in the atmosphere and most of the absorption at the Earth's surface. Evapotranspiration (LE) and sensible heat fluxes (H) transfer much of the absorbed solar energy to the atmosphere. The absorbed solar energy must ultimately be returned to space as thermal infrared radiation as indicated on the right side. Only the net thermal flux between the surface and atmosphere is shown. Reductions of thermal flux to space from increasing concentrations of trace gases warm the global atmosphere.

What is surprising is that other atmospheric gases, present in minute amounts, in some cases in concentrations <1 part per 10^9 (p.p.b.), also contribute significantly to this trapping of thermal radiation. These gases include, in particular, carbon dioxide, tropospheric ozone, methane, nitrous oxide, and certain chlorocarbons, in order of their present contributions to atmospheric radiative processes. Without the atmosphere's radiatively active constituents, the Earth would lose thermal radiation essentially as a black body at the temperature of its surface, $T_s = 287.5$ K, that is, ~387 W m^{-2}, neglecting corrections for the nonlinearity of the black-body emission, surface emissivities <1, and stratospheric effects. The actual radiative flux from the top of the atmosphere is 239 W m^{-2}, so the total amount of trapped radiation is ~148 W m^{-2}. Sustained changes in this trapping by as little as 1 W m^{-2} change the Earth's radiative balance sufficiently to be of considerable importance for the climate system. Table 1 shows the current concentrations of atmospheric trace gases and contributions to this radiative trapping.

Table 1 The current 1985 trapping of thermal infrared radiation (ΔQ) by current tropospheric trace constituents

Gas	Current concentration	ΔQ_{total} (W m^{-2})	Ref.
Carbon dioxide	345 p.p.m.	~50	63
Methane	1.7 p.p.m.	1.7	16
Ozone	10–100 p.p.b.	1.3	
Nitrous oxide	304 p.p.b.	1.3	16
CFC-11	0.22 p.p.b.	0.06	19
CFC-12	0.38 p.p.b.	0.12	19

The term ΔQ_{total} is the change of net radiation at the tropopause if the given constituent is removed, but the atmosphere is otherwise held fixed.

The contribution to the Earth's thermal budget of such minute concentrations of trace gases is of considerable interest in its own right. However, the changing concentrations of these gases as a result of human activities[20,21] add a considerable sense of urgency to their study. We review here our current understanding

of the radiative properties of the relevant gases, their sources, sinks, and changing concentrations, and the implications of these changes for future climate.

Radiative properties of the atmosphere

Solar radiation of wavelengths from ~0.3 to ~4 μm heats the climate system. Thermal emission at wavelengths from ~4 to ~100 μm, in turn, cools the Earth's surface and atmosphere, ultimately returning the absorbed solar energy to space. The solar radiation is scattered (reflected in all directions) by clouds, aerosols, the Earth's surface, and the major atmospheric molecules (Fig. 1) and absorbed by all but the last of these. Thick clouds act nearly as black bodies in absorbing and emitting thermal infrared radiation, as do also most terrestrial surfaces (an exception is quartz sand with relatively low emissivities[22]).

Of the radiatively active gases in the current atmosphere, only H_2O, CO_2, CH_4, O_3, N_2O and the chlorofluorocarbons (CFC-11 and CFC-12) are in sufficient concentrations to be important in Earth's overall thermal budget. Of these, the strongest absorber by far is water vapour. Indeed, much of tropospheric radiation can be described with water vapour as the only gaseous absorber. Water in either vapour or in cloud form absorbs solar radiation and absorbs and emits thermal radiation. These water vapour states are internal to the climate system, that is, their distributions are controlled by climate processes themselves (that is, the atmospheric hydrological cycle) rather than by sources uncoupled to the climate system. Understanding how water vapour concentrations and cloud radiative properties might change in the future thus requires knowledge of how these terms function as feedbacks in the climate system (a question we shall return to later). Our primary thrust here is to review the role of the other less-abundant trace gases, whose concentrations are being directly perturbed by human activities. Understanding the radiative properties of these gases and their future concentrations is the key to understanding the relative contributions of these gases to climate change.

Ozone is the only other atmospheric gas which absorbs much solar radiation, primarily in the stratosphere. Atmospheric carbon dioxide is but a very weak absorber of solar radiation. The other atmospheric trace gases only affect the atmospheric heat budget through their absorption and emission of the thermal infrared radiation, primarily over the wavelength range ~6–16 μm. Furthermore, at the wavelengths where water vapour strongly absorbs and emits radiation, the effect of other gases is minimal. The vibrational-rotational bands of water vapour thus block radiation at wavelengths <8 μm and rotational bands block wavelengths >18 μm. Carbon dioxide, in turn, dominates the absorption of radiation between 12 and 18 μm.

The remaining spectral region from 8 to 12 μm is known as the 'window' because of the atmosphere's relative transparency to radiation over these wavelengths. The intensity of black-body radiation depends on wavelength according to the Planck function; at the temperatures of the Earth's surface, this function has its maximum values in the window region. Consequently, ~25% of the thermal emission from the Earth's surface (~100 W m^{-2}) is at wavelengths of 8–12 μm. A larger fraction of the emission from the top of the atmosphere is in this spectral range. In this wavelength region, emission varies with temperature T approximately as $\exp(-1{,}500/T)$. A trace gas at a temperature ~33 °C less than that of Earth's emission temperature will thus only re-emit about half as much energy as it absorbs. Because of the presence of clouds, the maximum increase of trapping in the window region is ~30 W m^{-2}.

Interestingly enough, CH_4, O_3, N_2O, CFC-11 (CCl_3F) and CFC-12 (CCl_2F_2) all have strong absorption bands in the atmospheric window region. These trace gases absorb and emit as functions of wavelength in discrete lines with extended wings. These lines occur in bands and result from the rotational splitting of individual vibrational energy transitions of the molecules. Their strength is determined from the strength of the band transitions, from the concentration of the trace gas, and from the rotational partitioning of the band into individual lines. The emission rate of a line depends on its absorption strength and on local atmospheric temperature.

The weakest lines absorb radiation significantly only in their line cores, and this absorption increases essentially linearly with concentration of the absorber gas. Somewhat stronger lines absorb radiation mostly in the wings, with only relatively small amounts absorbed by their saturated cores. Increasing absorber concentration pushes the peak absorption farther into the line wings so that wing absorption increases with the square root of the product of atmospheric pressure and absorber concentration. With even stronger line strengths, the peak absorption is pushed so far into line wings that other lines within the band overlap the absorbing wings and absorption only increases logarithmically with increasing absorber concentration. The absorption of a band varies with absorber concentration according to the variation of its stronger absorbing lines.

The chlorofluorocarbons CFC-11 and CFC-12 and tropospheric ozone are present in such small concentrations and have so many individual lines that their absorption of thermal radiation is nearly proportional to their concentration. Methane and nitrous oxide, being relatively more abundant, increase their absorption essentially according to the square root of their concentrations, whereas carbon dioxide absorption is proportional to the logarithm of its concentration. All the trace gases absorb not in single bands but in multiple bands, and weaker hot and isotopic bands are also present. The above scaling arguments are only approximate and are especially prone to error if applied to large changes in concentration where either the stronger bands may change their dependence on absorber amount, or previously unimportant weaker bands of a given gas may become relatively more important.

Increases in the concentrations of atmospheric trace gases since pre-industrial times and the consequent trapping of thermal radiation are shown in Table 2. The trapping by ozone and the CFCs, whose stronger bands are in the middle of the window region, is affected very little (~15%) by overlap with water vapour and with carbon dioxide absorption. Methane and nitrous oxide, whose strongest bands are on the short wavelength edge of the window region, lose about half of their trapping[20] by such overlap. Since much of the effect of increases in the trace gases is to make the atmospheric window region more opaque, this trapping might be called the 'dirty window' effect.

Table 2 Estimated pre-industrial trace gas concentrations and implied change in thermal trapping to 1985

Gas	Pre-industrial concentration	$\Delta Q_{\text{pre-industrial}}$ (W m^{-2})
Carbon dioxide	275 p.p.m.	1.3
Methane	0.7 p.p.m.	0.6
Tropospheric ozone (below 9 km)	0–25% less	0.0–0.2
Nitrous oxide	285 p.p.b.	0.05
CFC-11	0.00 p.p.b.	0.06
CFC-12	0.00 p.p.b.	0.12
Total		~2.2

Trapping is inferred from refs 19 and 20, scaling approximately logarithmically, with CO_2 concentration, with the square root of N_2O and CH_4 concentration, and linearly with O_3 and CFC-11 and -12 concentrations.

Atmospheric trace gases

Carbon dioxide: Atmospheric carbon dioxide concentrations are now ~25% higher than they were 200 yr ago before the age of extensive industrialization and forest clearing. Current concentrations (1985) are about 345 p.p.m. (parts per 10^6) and are increasing by 1–1.5 p.p.m. yr^{-1}, mostly as a result of continued

burning of fossil fuel (adding $\sim 5.2 \times 10^{12}$ kg yr^{-1} of carbon) and forest removal (continuing to add about 10^{12} kg yr^{-1} of carbon)[10]. The basic features of the global carbon cycle are well known, but questions remain as to the contributions of land soils and forests and the rate of uptake of carbon by the oceans. The largest source of uncertainty in projecting future atmospheric carbon dioxide concentrations, however, lies in the future rates of fossil fuel combustion.

Halocarbons: Halogenated hydrocarbons (halocarbons) are now widely produced and widely used. These include fluorocarbons, chlorofluorocarbons, chlorocarbons and bromocarbons. Most scientific attention has focused on the potential role of chlorine and bromine atoms from these molecules as ozone-destroying catalysts in Earth's stratosphere[23-25]. Certain of these chemicals have also been recognized to be potent greenhouse gases[11,20].

The chlorofluorocarbons, often referred to popularly by their trade name of 'Freons', CCl_3F (CFC-11) and CCl_2F_2 (CFC-12), were measured first in the atmosphere in 1971 (ref. 26) and 1973 (see, for example, ref. 27), respectively. Since then, increasingly accurate and precise measurements have shown that their atmospheric concentrations have grown at about the same rate as would be expected from industrial production and release into the atmosphere[24,28], after minor corrections for the amounts produced but not yet released and for the quantities destroyed in the stratosphere and dissolved in oceans. In 1981, there were about 6.0×10^9 kg of CFC-12 in the atmosphere together with 5.0×10^9 kg of CFC-11. At 1981 release rates, these amounts represent the cumulative results of 15–20 yr of global emissions. (Unpublished data from several investigators give 1985 mixing ratios of CFC-11 of at least 0.22 p.p.b. and for CFC-12 of at least 0.38 p.p.b.). Indeed, atmospheric concentrations of these compounds were observed to have increased by $\sim 6\%$ yr^{-1} during 1978–81 (refs 29, 30). In the early 1970s, annual emissions were a larger fraction of the amounts already in the atmosphere, and larger percentage annual increases were observed, along with considerably more CFCs in the Northern Hemisphere than in the Southern Hemisphere. Although most of the release continues to be in the Northern Hemisphere, the hemispheric difference has decreased to $<10\%$.

A projection of concentrations of atmospheric CFC-11 and CFC-12 beyond the present requires some knowledge about future industrial production and release rates. Current releases annually increase mixing ratios of CFC-11 by about 12 p.p.t. (parts per 10^{12}) and CFC-12 by 21 p.p.t., as estimated from changing atmospheric concentrations. A recent report[31] attempts to estimate their future production and release rates and that of several other similar chemicals; it recognizes the dynamics of changing industrial usages, competitive products and world and regional populations. Worldwide CFC-11 emissions are projected to increase by between 2.8 and 5.1% yr^{-1} from 1980 until 2000; corresponding figures for CFC-12 are 2.5–3.5% yr^{-1}. Between AD 2000 and 2025, CFC-11 emissions could change by -1% to $+4.7\%$ yr^{-1} and CFC-12 emissions would increase by between 1.0 and 4.6% yr^{-1}. Beyond the year 2025, growth estimates are less well-based, but Quinn *et al.*[31] suggest annual increases of 0.6–2.0% for CFC-11 and 1.1–2.1% yr^{-1} for CFC-12.

Even if future release rates of CFC-11 and CFC-12 remained at present levels, their atmospheric concentrations would continue to increase for the next century because of the relatively long residence times, τ, for these species, at least 60 and 100 yr, respectively[32]. In general, for a well-mixed chemical with sources $S(t)$

$$\frac{dN(t)}{dt} = S(t) - N(t)/\tau \qquad (1)$$

where $N(t)$ is the total number of molecules (or mass) of the given species in the global atmosphere at time t. Even if we were to assume that present emissions remained constant, equation (1) shows that concentrations of CFC-11 and CFC-12 would more than double, to values of ~ 0.5 and 1.0 p.p.b. respectively, within the next 40 yr and eventually rise to values of ~ 0.7 and 2.1 p.p.b., using 60- and 100-yr lifetimes, respectively.

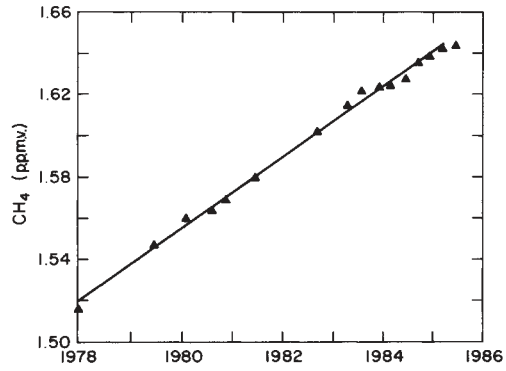

Fig. 2 Globally averaged methane concentrations in surface air from January 1978 to June 1985 as measured by Blake and Rowland[42]. Air samples were collected simultaneously from northern and southern latitudes. In computing global averages, measured values were weighted by the Earth's area in latitude belts. In 1985, there are 4.8×10^{15} g CH_4 in the atmosphere; annual sources (sinks) are $(3\text{–}7) \times 10^{14}$ g.

Other halocarbons requiring attention include CCl_4, $CClF_3$, CF_4, $CHClF_2$, $CHCl_2F$, $C_2H_3Cl_3$, $C_2Cl_3F_3$, $C_2Cl_2F_4$, C_2ClF_5, C_2F_6, $CBrF_3$ and $CBrClF_2$. Because of the location of the absorption bands of these species and their rapid rates of accumulation in the atmosphere, they represent potentially important greenhouse gases. Research is needed to quantify their band absorbances and atmospheric concentrations with special attention to $CHCl_2F$ and $C_2Cl_3F_3$.

Nitrous oxide: Atmospheric N_2O is increasing in concentration globally, although the record of its past change is not as extensive as that for methane, and the reasons for this increase are less clear than those for halocarbons. Weiss[33] measured a global increase of ~ 0.6 p.p.b. yr^{-1} (0.2% yr^{-1}) between 1976 and 1980, whereas Khalil and Rasmussen[34] find an 0.8 p.p.b. yr^{-1} increase between 1979 and 1982. The mid-1980 N_2O concentration in the Northern Hemisphere was 301 p.p.b. and in the Southern Hemisphere it was ~ 0.8 p.p.b. less. Weiss fits his 1976–80 data with one of two curves; either one that assumes an added combustion source of N_2O growing at 3.5% yr^{-1} or one that assumes an agricultural-fertilizer source growing at 6% yr^{-1} (ref. 33) with an atmospheric residence time of 100 yr in both cases. Weiss, in extending his N_2O monitoring through 1984, finds that global concentrations continue to rise by 0.6 p.p.b. yr^{-1} (personal communication), but that it is not yet possible to distinguish between the two source-growth curves that fit the data. Earlier data from 1961–74 showed similar rates of N_2O increase[35].

Although the present observed and projected rates of N_2O increase may seem small, they imply that total global sources of N_2O are now elevated by $\sim 30\%$ over unperturbed steady-state sources, assuming a growth rate of 0.2% yr^{-1} and a 150-yr lifetime for N_2O. If the N_2O increase is due to either increased microbial nitrification and denitrification of agricultural fertilizers, or combustion, then much of this imbalance has developed in the past few decades and it may continue to grow rapidly.

Concentrations of N_2O of 320–330 p.p.b. are likely by AD 2000, regardless of which anthropogenic source is assumed to be growing[33,34]. Better future projections require determination of whether increased combustion of nitrogen-containing fuels[36,37] and biomass[21] or increased application of nitrogen fertilizers[38] is primarily responsible for the continuing N_2O increase. Both sources are difficult to quantify; field losses of N_2O due to microbial nitrification and denitrification of nitrogen fertilizers are variable[38,39] and candidate elementary reactions

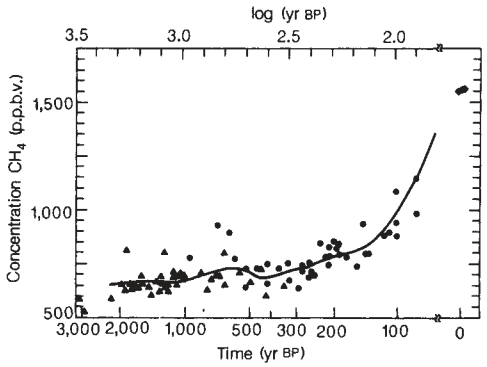

Fig. 3 Concentrations of atmospheric methane (100–300 yr BP) from ref. 44. ●, Data from polar ice cores obtained from Greenland; ▲, data from ice cores at the South Pole. The present concentration of methane is shown on the right (◆). The solid line is the smoothed average concentration based on the data; it is the average concentration in successive overlapping periods of 0.3 units each in the log (l) scale at the top of the figure.

that can produce N_2O in combustion have been identified only recently[40].

Methane: Methane is of considerable scientific interest because of its relatively rapid growth and the diverse possible causes of this increase. Global concentrations have increased by $>1\%$ yr^{-1} since 1978, as shown by Fig. 2, based on data from flame-ionization gas chromatography. A reanalysis[41] of ground-based solar absorption infrared spectroscopic data concludes that the concentration of tropospheric CH_4 in 1951 was 1.15 p.p.m., about 30% below that of 1985 (ref. 42). An earlier re-examination of infrared data from the 1950s and 1960s had concluded[43] that the rate of methane increase was slower.

The increase in global methane apparently began in previous centuries. Figure 3 shows an analysis of gases trapped in dated ice cores[44], indicating that methane concentrations have doubled since the eighteenth century, but that they were relatively constant for the previous 2,000–3,000 yr. Selective diffusion of CH_4 out of old ice cores may have biased the data of Fig. 3 (ref. 43), but H. B. Craig, who earlier found similar results[45], considers this unlikely (personal communication) based on his tests. Further confirmation has been reported[46]. Methane-consuming microbes may have lived in the ice, but we consider this unlikely.

Why has atmospheric methane increased in the past, and what is its future? Answering these questions requires knowledge of both the sources and sinks of methane. Ehhalt[47] summarized five measurements of ^{14}C in samples from air liquefication plants in the 1950s. These samples had a ^{14}C content of about 80% of that of standard wood, or equivalently 20% 'dead carbon' from fossil fuels. He suggested that this value of 20% should only be used as an upper limit since air liquefication plants are usually situated in heavily industrialized areas so that the samples were subject to contamination from local fossil-fuel-derived methane. Various authors over the past decade have constructed methane-source inventories subject to this constraint. A recent examination[21] lists rice paddies, ruminant animals, biomass burning, swamps and marshes, natural gas, and coal mining losses as the major sources, in decreasing order of importance. However, serious questions of mechanisms and related ecological variability remain[48–51]. Further, we should be cautious about conclusions drawn from the 1950s ^{14}C data because: first, the relative sizes of ^{14}C-rich and ^{14}C-poor sources are probably changing with time; and second, the old samples, collected by liquefying air, may not be representative of the $^{14}CH_4/^{12}CH_4$ in air. Unfortunately, few conclusions can be drawn about methane sources from ^{14}C analyses today in view of the bomb-produced ^{14}C in the contemporary biota and sediments. It might be useful to examine the concentrations of the ^{13}C stable isotope; such research is just beginning[52].

The principal known sink of atmospheric methane is the gas-phase reaction $OH + CH_4 \rightarrow CH_3 + H_2O$ (ref. 72). Some tantalizing but indirect evidence suggests that atmospheric OH concentrations are decreasing[53], at least in NO poor regions—the lower and middle troposphere; increasing methane and increasing CO concentrations (not yet proven) should act to suppress OH (ref. 54) through nonlinear atmospheric chemistry.

Ozone: Ozone is of considerable interest because of its important roles, its complex behaviour, and its susceptibility to human-induced global change. Near the ground in urban areas, ozone is a pollutant. Throughout the global troposphere, ozone photolysis initiates free-radical chemistry. In the middle and upper stratosphere, where the largest concentrations are found, ozone strongly attenuates solar ultraviolet light and in doing so drives stratospheric wind systems.

Tropospheric ozone increases are difficult to discern with extant observing systems, but increases have been indicated. A recent critical analysis[55] of ozone data finds that, on average over Europe and North America from the late 1960s to the early 1980s, near-surface ozone has increased by 1–3% yr^{-1} and ozone in the middle troposphere (700–500 mbar) by 1–2% yr^{-1}. These increases occur largely during the summer, especially in industrialized areas. Such increases might have begun in the 1940s, as is suggested by shifts in the seasonal cycle of ozone concentrations and other scattered observations[55]. There is considerable variability and little evidence for change in the upper troposphere.

Theoretical models of tropospheric chemistry predict that increasing anthropogenic releases of hydrocarbon and nitrogen oxide (NO_x) gases should be increasing tropospheric ozone[55–57,15]. Such increases depend on poorly known atmospheric NO_x concentrations and on some meteorological processes such as vertical transport and chemical roles of clouds, but changes in the Northern Hemisphere should be larger than those in the Southern Hemisphere, as is evidently observed. Future changes in the stratosphere may also lead to increases of tropospheric ozone.

As discussed previously[20], most studies of the latitudinal variation of tropospheric ozone indicate that concentrations in the Northern Hemisphere are at least 50% higher than in the Southern Hemisphere. However, a recent aircraft survey has given contradictory results[58], possibly because of seasonal or longitudinal variations. Furthermore, latitudinal variations may be due to transport[59].

An association of observed trends of ozone in the Northern Hemisphere with increases in total fossil fuel use would also support the possibility of an increase of tropospheric ozone in the Northern Hemisphere of up to 50% over pre-industrial values. We indicate in Table 2 that global average tropospheric ozone (below 9 km) is estimated to have increased by between 0 and 25% since pre-industrial time. Improving estimates of past or future ozone change will require a better understanding of the contributions of ground and high-level pollution.

Global stratospheric ozone changes are likely to occur because of continuing and accelerating human activities[24,25]. Increasing concentrations of chlorofluorocarbons and nitrous oxide decrease stratospheric O_3 at altitudes above 30 km. Changes of ozone in the lower stratosphere are more complex and difficult to project; they will depend on latitude and altitude and on wind systems[59,60]. A variety of chemical reactions involving polyatomic species (many of which have yet to be measured in the atmosphere) also affect this response.

Future scenarios

For comparing the future climate effects of the various trace gases, we take the year 2050 as a reference point and assume the ranges indicated in Table 3. The question of possible future concentrations for CO_2 has been extensively studied, and we have adopted values from the latest such study[10].

A range of possible future emissions for CFC-11 and CFC-12 has been obtained from economic analysis[31], and we have used

these emissions together with equation (1) to obtain the concentrations shown in Fig. 4. Concentration scenarios have taken $\tau = 60$ yr for CFC-11 and $\tau = 100$ yr for CFC-12, near the low end of most previously inferred values[32]. Lifetimes are likely to lie in the range 50–80 yr and 90–130 yr, respectively. These lifetimes will decrease in the future, as increased concentrations of chlorine atoms lower the ozone concentrations above 30 km, and hence increase the fluxes of ultraviolet that photolyse the CFCs. Obvious decreases in the total column ozone following stratospheric ozone decrease are likely to trigger political constraints on further increases in the production of the CFCs. Our projections neglect the uncertainty in CFC lifetimes and their decrease with increasing burden and also neglect possible emission reductions from future regulation of CFC production.

Table 2 shows that the radiative effect of the CFCs which have been added to the atmosphere up to 1985 is only ~11% of that from CO_2 increases. However, the CO_2 increase has occurred over the past two centuries, and the current burden of CFCs has been added almost entirely within the past 30 yr. The radiative effect of these CFCs added over the past 30 yr is about one-third that of the CO_2 added over the same period. Table 3 indicates that for the assumed future scenario the additional radiative trapping by the CFCs between 1985 and 2050 is likely to be ~70% that of CO_2. This increase in the relative importance of the CFCs in the future follows from the near-linear dependence on concentration of the CFC radiative effects versus the logarithmic dependence of the effects of CO_2.

Because of our current relatively poor understanding of the reasons for the increases in methane concentrations, a wide range of possible futures appears in Table 3. A continuation of the current growth rate of 1.2% yr^{-1} to the year 2050, assuming present methane lifetimes, would give 3.7 p.p.m. at that time. Increases in methane will probably be amplified by decreasing OH, but will be diminished by slowdown in population growth and required resources. Another recent analysis[21] argues that increases from pre-industrial concentrations are likely to be proportional to projected future populations. They accordingly infer concentrations of 2.5 p.p.m. by 2050; values this small would require a large reduction in methane growth rates within the next few decades. We judge that in the year 2050 concentrations will lie between 2.1 and 4.0 p.p.m. The upper limit is inferred from the extrapolation of current growth plus a small decrease (8%) of methane lifetimes. Methane lifetimes may decrease by much more[54]. The lower limit is inferred by arguing that the current trend should last at least 20 yr but that, considering our ignorance of the processes involved, we cannot exclude absence of further growth after that. Table 3 suggests that from now to 2050 the radiative effects of increasing methane are likely to be about one-quarter that of CO_2. Table 2 indicates that the increase in radiative trapping from past methane increases has been about the same as that expected from future methane increases and is about half of that inferred from past CO_2 increases. Methane has already increased to ~250% of pre-industrial values and probably will not repeat this relative increase by 2050. The relative increase of CO_2, on the other hand, will probably be greater in the next 65 yr than it has been up to now[10].

If the anthropogenic source of nitrous oxide were to continue to grow at 3.5% yr^{-1}, it would increase by a factor of 10 by the year 2050 and N_2O concentrations would rise above 500 p.p.b. (ref. 33). Such rapid future growth is probably excluded by economic and population constraints[21]. Assuming that a quadrupling of the current emission rates over the next 65 yr is not impossible, we infer an upper limit for N_2O concentrations of 450 p.p.b. for the year 2050. We infer a lower limit of 350 p.p.b. for the year 2050 using an average annual increase similar to that now observed.

A likely upper limit to fossil-fuel consumption over the next century is about four times current consumption rates[10]. With such consumption and an upper limit of 20% of current ozone associated with fossil-fuel pollution, global tropospheric ozone could conceivably increase by 60% over current values. Ozone will also increase in the upper troposphere and lower stratosphere in response to increases of the CFCs and to oxides of nitrogen from increasing jet aircraft traffic. The details of latitudinal and especially vertical distribution of ozone change are important for any accurate estimate of climate effects. Lacking such details, we estimate the likely radiative trapping of changing ozone concentrations by the year 2050 as that given by a change in ozone between 0 and 50% uniformly over the altitude range 0–12 km.

To determine the net contribution to radiative trapping included in Table 3, we have simply summed separately the upper and lower limits of the projected contributions of the individual gases. Although all contributions are unlikely to achieve their upper or lower limits simultaneously, this assumption probably does not overestimate the likely range of total trapping for two reasons. First, the rates of increase of the different trace gases are more likely to be highly correlated than not—their sources all depend heavily on fossil-fuel utilization; methane and nitrous oxide emissions both also depend on agricultural development and that of the CFCs on general technological development. Second, past experience with similar uncertain environmental questions indicates that actual uncertainties are likely to be larger than can be judged from simple arguments such as those used here. In particular, there are many other trace gases present in small but rapidly growing concentrations[20], some of which will add significantly to global warming by the year 2050.

Table 3 Scenario for trace gas concentrations in the year 2050 and implied increased trapping of thermal radiation from 1985 (ref. 19)

Gas	Year 2050 scenario	ΔQ_{2050} (W m^{-2})
Carbon dioxide	400–600 p.p.m.	0.9–3.2
Methane	2.1–4.0 p.p.m.	0.2–0.9
Tropospheric ozone (0–12 km)	15–50% more	0.2–0.6
Nitrous oxide	350–450 p.p.b.	0.1–0.3
CFC-11	0.7–3.0 p.p.b.	0.23–0.7
CFC-12	2.0–4.8 p.p.b.	0.6–1.4
Total		2.2–7.2

Referring to either the lower or the upper limit totals in Table 3, we infer that the total contribution of the other trace gases is more likely than not to exceed the contribution from CO_2.

Implications for climate change

We have aimed to provide an overall framework for considering the relative contributions of various trace gases to climate change. Relatively realistic three-dimensional climate models have been used to study only a very limited number of scenarios for future climate; that is, scenarios assuming a steady-state doubling or quadrupling of atmospheric carbon dioxide concentrations. The radiative forcing for the latter is about double that for the former.

The future climate change from likely increases of all trace gases will undoubtedly differ in detail from that inferred from the superposition of the climate changes that would occur, assuming that each trace gas changes separately. Furthermore, the climate change from individual trace gases depends not only on the global average trapping of radiation as discussed here, but also on the latitudinal and especially vertical distributions of atmospheric heating or cooling changes implied by the trace gas change. However, the implications of these details have not yet been satisfactorily resolved, and so our estimates of the climate change resulting from the various trace gases assume that the dependence of this climate change on external forcing can simply be represented by the global radiative trapping alone.

Indeed, the radiative trapping values given in Tables 1–3 are only approximate estimates. Their precise values depend not only on (somewhat uncertain) band strengths but also on the temporally and spatially varying distributions of cloudiness and atmospheric temperatures. The values used here have been inferred mostly from simple one-dimensional models of the atmosphere. Recognizing these caveats, we suggest that at present the most useful way to estimate the future climate change from CO_2 and the other trace gases is to scale from the studies that have been done on climate change from CO_2 increases, allowing for the time lag required for the oceans to warm up.

Three-dimensional general circulation models (GCMs) represent the climate system as the sum of the day-to-day weather systems integrated over many years of simulated time. In doing so, they can include realistically all the feedbacks of simpler models plus those that depend on the details they generate. They include, in particular, albedo feedbacks from seasonally varying snow and sea ice, lapse rate feedbacks involving adjustment to moist adiabatic lapse rates in tropical latitudes, controls by baroclinic disturbances in mid-latitudes, and feedbacks by the highly stable stratification of polar latitudes. Cloud feedbacks are potentially very important for amplifying global temperature change, but they cannot be inferred yet with confidence, and negative feedbacks on solar radiation absorption from changes in cloud liquid water have not been included[61].

Because of the difficulty in isolating individual feedbacks in GCMs, and the expense of examining all trace gases of possible significance, simpler energy balance[62] and convective adjustment models[63] have also proved valuable.

Recent GCM simulations[3,6,7] give for steady-state CO_2 doubling ($\Delta Q \simeq 4.0\ W\ m^{-2}$) a global average temperature increase of between 2.1 °C (ref. 3) and 4.8 °C (ref. 6). Consideration of uncertain model feedbacks suggests that a value as low as 1.5 °C or as high as 5.5 °C is possible[10].

Because several decades or more are required for the oceans to equilibrate with changes in global radiation[64–69], we cannot convert the heating rates given in Tables 2 and 3 directly into expected temperature changes for the same dates. However, continuing the current burden of trace gases added by human activities indefinitely implies an eventual increase from pre-industrial temperatures of 0.5–2° C. Global mean temperatures can only be estimated with any confidence back to 1900. About two-thirds of the anthropogenic forcing has developed since that time. Oceanic thermal inertia is currently reducing the temperature response by (very roughly) half of what it would be in a steady state. Allowing for this factor, we infer a temperature increase of 0.3–1.0 °C from 1900 to the present[10,70]. The observed increase is about 0.5 °C (refs 10, 70) which would seem to confirm the present analysis. However, global temperatures around 1940 were nearly as warm as now and they declined in the 1960s. Thus, unexplained climate variations occur that will probably confound unambiguous identification of the trace gas signal for at least another decade or two.

The scenarios given in Table 3 imply that by the year 2050 there will be a global average temperature increase of 1 °C to >5 °C, depending on the extent of positive feedbacks in the climate system and on reduction of the response by oceanic heat uptake. Global temperatures will probably continue to grow well into the twenty-second century as the atmospheric loading of trace gases and ocean heat content increases further.

The GCMs simulate not only global conditions but also the detailed geographical distribution of many climate parameters including the atmospheric hydrological cycle. Implications of future climate change from trace gases for agriculture and natural ecosystems require establishing these details with some confidence. All the GCM simulations indicate largest temperature changes in high latitudes. Some models strongly suggest a significant mid-latitude, mid-continent summer drying. Past model studies have inspired a wide range of climate-impact 'what if' studies, examining the potential implications of the

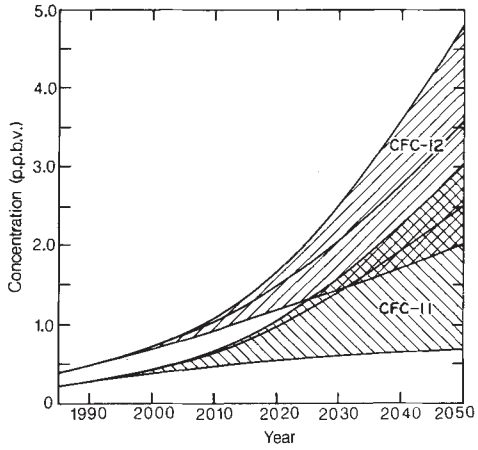

Fig. 4 Range of possible scenarios of the concentrations of CFC-11 and CFC-12 between 1985 and 2050 as inferred from future sources projected from an economic analysis[31]. Upper, lower and middle scenarios are shown for each gas and their ranges are indicated by the slanted line patterns.

range of possible future climates[73]. However, practical analyses will require a new generation of climate models whose global feedbacks and regional simulations can be accepted with confidence. They will also require allowance for the large-scale adjustments of human systems that can occur on the timescales involved[71].

Accurate model predictions may take more than a decade to arrive. Meanwhile, further emphasis should be given to defining and bounding the uncertainties in future climate change[71]. Without a better understanding of the extreme upper limits to possible future climate change, we must view with considerable concern this global experiment now under way.

We thank Drs J. Kiehl, W. Clark, and P. Crutzen for helpful comments. The National Center for Atmospheric Research is sponsored by the NSF.

1. Callendar, G. S. *Q. Jl R. met. Soc.* **64**, 223–240 (1938).
2. Manabe, S. & Wetherald, R. T. *J. atmos. Sci.* **24**, 241–259 (1967).
3. Manabe, S. & Stouffer, R. J. *J. geophys. Res.* **85**, 5529–5554 (1980).
4. Climate Research Board *Carbon Dioxide and Climate: Scientific Assessment* (National Academy of Sciences, Washington DC, 1979).
5. Dickinson, R. E. *Carbon Dioxide Review 1982* (ed. Clark, W. C.) 101–133 (Oxford University Press, 1982).
6. Hansen, J. *et al. Maurice Ewing Symp. 5* (eds Hansen, J. & Takahashi, T.) (American Geophysical Union, Washington DC, 1984).
7. Washington, W. M. & Meehl, G. A. *J. geophys. Res.* **89**, 9475–9503 (1984).
8. Carbon Dioxide Assessment Committee *Changing Climate* (National Academy of Sciences, Washington DC, 1983).
9. Mitchell, J. F. B. *Q. Jl R. met. Soc.* **109**, 112–152 (1984).
10. Bolin, B., Döös, B. R., Jager, J. & Warrick, R. A. (eds) *The Greenhouse Effect, Climatic Change and Ecosystems. A Synthesis of the Present Knowledge* (Wiley, Chichester, in the press).
11. Ramanathan, V. *Science* **190**, 50–52 (1975).
12. Wang, W. C., Yung, Y. L., Lacis, A. A., Mo, T. & Hansen, J. E. *Science* **194**, 685–690 (1976).
13. Dickinson, R. E., Liu, S. C. & Donahue, T. M. *J. atmos. Sci.* **35**, 2142–2152 (1978).
14. Flohn, H. *Carbon Dioxide, Climate and Society* (ed. Williams, J.) 227–238 (Pergamon, London, 1978).
15. Fishman, J., Ramanathan, V., Crutzen, P. J. & Liu, S. C. *Nature* **282**, 818–820 (1979).
16. Donner, L. & Ramanathan, V. *J. atmos. Sci.* **37**, 119–124 (1980).
17. Hameed, S., Cess, R. D. & Hogan, J. *J. geophys. Res.* **85**, 7537–7545 (1980).
18. Lacis, A., Hansen, J., Lee, P., Mitchell, P. & Lebedeff, S. *Geophys. Res. Lett.* **8**, 1035–1038 (1981).
19. World Meteorological Organization *WMO Global Ozone Research and Monitoring Project, Rep. No. 14 of the Meeting of Experts on Potential Climatic Effects of Ozone and Other Minor Trace Gases* (World Meteorological Organization, Geneva, 1982).
20. Ramanathan, V., Cicerone, R. J., Singh, H. B. & Kiehl, J. T. *J. geophys. Res.* **90**, D3, 5547–5566 (1985).
21. Bolle, H. J., Seiler, W. & Bolin, B. *The Greenhouse Effect, Climatic Change, and Ecosystems. A Synthesis of the Present Knowledge* Ch. 4 (Wiley, Chichester, in the press).
22. Prabhakara, C. & Dalu, G. *J. geophys. Res.* **81**, 3719–3724 (1976).
23. Molina, M. J. & Rowland, F. S. *Nature* **249**, 810–812 (1974).
24. National Academy of Sciences/National Research Council *Stratospheric Ozone Depletion by Halocarbons: Chemistry and Transport* (Washington DC, 1979).
25. Prather, M. J., McElroy, M. B. & Wofsy, S. C. *Nature* **312**, 227–231 (1984).
26. Lovelock, J. E., Maggs, R. J. & Wade, R. J. *Nature* **241**, 194–196 (1973).
27. Hester, N. E., Stephens, E. R. & Taylor, O. C. *J. Air Pollut. Control Ass.* **24**, 491–595 (1974).
28. Penkett, S. A., Brice, K. A., Derwent, R. G. & Eggleton, A. E. J. *Atmos. Envir.* **13**, 1011–1019 (1979).
29. Cunnold, D. M. *et al. J. geophys. Res.* **88**, C13, 8379–8400 (1983).
30. Cunnold, D. M. *et al. J. geophys. Res.* **88**, C13, 8401–8414 (1983).
31. Quinn, T. H. *et al. Projected Use, Emissions and Banks of Potential Ozone-Depleting Substances* WD-2483-1-EPA (Rand Corp., Santa Monica, 1985).

32. Stordal, F., Isaksen, I. S. A. & Horntveth, K. *J. geophys. Res.* **90**, D3, 5757-5776 (1985).
33. Weiss, R. F. *J. geophys. Res.* **86**, C8, 7185-7195 (1981).
34. Khalil, M. A. & Rasmussen, R. A. *Tellus* **35B**, 161-169 (1983).
35. Craig, H., Weiss, R. F. & Dowd, W. L. *Pap. at Symp. on the Terrestrial Nitrogen Cycle and Possible Atmospheric Effects* (American Geophysical Union, Washington DC, 1976).
36. Pierrotti, D. & Rasmussen, R. A. *Geophys. Res. Lett.* **3**, 265-268 (1976).
37. Weiss, R. F. & Craig, H. *Geophys. Res. Lett.* **3**, 751-754 (1976).
38. Delwiche, C. C. (ed.) *Denitrification, Nitrification, and Atmospheric Nitrous Oxide* (Wiley, New York, 1981).
39. Mosier, A. R., Parton, W. J. & Hutchinson, G. L. *Environmental Biogeochemistry* (ed. Hallberg, R.) (1982).
40. Perry, R. A. *J. chem. Phys.* **82**, 5485-5488 (1985).
41. Rinsland, C. P., Levine, J. S. & Miles, T. *Nature* **318**, 245-249 (1985).
42. Blake, D. R. & Rowland, F. S. *J. atmos. Chem.* (in the press).
43. Ehhalt, D. H., Zander, R. J. & Lamontagne, R. A. *J. geophys. Res.* **88**, C13, 8442-8446 (1983).
44. Rasmussen, R. A. & Khalil, M. A. K. *J. geophys. Res.* **89**, D7, 11599-11605 (1984).
45. Craig, H. & Chou, C. C. *Geophys. Res. Lett.* **9**, 1221-1224 (1982).
46. Stauffer, B., Fischer, G., Neftel, A. & Oeschger, H. *Science* **229**, 1386-1387 (1985).
47. Ehhalt, D. H. *Tellus* **26**, 58-70 (1974).
48. Rasmussen, R. A. & Khalil, M. A. K. *J. geophys. Res.* **86**, C10, 9826-9832 (1981).
49. Cicerone, R. J., Shetter, J. D. & Delwiche, C. C. *J. geophys. Res.* **88**, C15, 11022-11024 (1983).
50. Seiler, W., Holzapfel-Pschorn, A., Conrad, R. & Scharfe, D. *J. atmos. Chem.* **1**, 241-268 (1984).
51. Harriss, R. C., Gorham, E., Sebacher, D. I., Bartlett, K. B. & Flebbe, P. A. *Nature* **315**, 652-654 (1985).
52. Stevens, C. M. & Rust, F. E. *J. geophys. Res.* **87**, C7, 4879-4882 (1982).
53. Khalil, M. A. K. & Rasmussen, R. A. *Atmos. Envir.* **19**, 397-407 (1985).
54. Thompson, A. M. & Cicerone, R. J. *Nature* (submitted).
55. Logan, J. A. *J. geophys. Res.* **90**, 10463, 10482 (1985).
56. Liu, S. C., Kley, D., McFarland, M., Mahlman, J. D. & Levy, H. II *J. geophys. Res.* **85**, 7546-7552 (1980).
57. Crutzen, P. J. & Gidel, L. T. *J. geophys. Res.* **88**, 6641-6661 (1983).
58. Gregory, G. L., Beck, S. M. & Williams, J. A. *J. geophys. Res.* **89**, 9642-9648 (1984).
59. Levy, H., Mahlman, J. D., Moxim, W. J. & Liu, S. C. *J. geophys. Res.* **90**, 3753-3772 (1985).
60. Isaksen, I. S. A. & Stordal, F. *J. geophys. Res.* **90** (in the press).
61. Somerville, R. C. J. & Rener, L. A. *J. geophys. Res.* **89**, 9668-9672 (1984).
62. North, G. R., Cahalan, R. G. & Coakley, J. A. *Rev. Geophys. Space Phys.* **19**, 91-122 (1981).
63. Ramanathan, V. & Coakley, J. A. *Rev. Geophys. Space Phys.* **16**, 465-489 (1978).
64. Bretherton, F. P. *Prog. Oceanogr.* **11**, 93-129 (1982).
65. Spelman, M. J. & Manabe, S. J. *J. geophys. Res.* **89**, 571-586 (1984).
66. Bryan, K., Komro, F. G., Manabe, S. & Spelman, M. J. *Science* **215**, 56-68 (1982).
67. Thompson, S. L. & Schneider, S. H. *Science* **217**, 1031-1033 (1982).
68. Schneider, S. H. & Thompson, S. L. *J. geophys. Res.* **6**, 3135-3147 (1981).
69. Wigley, T. M. L. & Schlesinger, M. E. *Nature* **315**, 646-652 (1985).
70. Wigley, T. M. L. *Climate Monitor* **13**, 133-148 (1985).
71. Clark, W. C. *Ecologically Sustainable Development of the Biosphere* (Publ. No. 26, IIASA, 1985).
72. Crutzen, P. J. *The Geophysiology of Amazonia* (ed. Dickinson, R. E.) Ch. 8 (Wiley, New York, in the press).
73. Parry, M. L. (ed.) *Climatic Change* (Spec. Issue) **7** (1985).

ARTICLES

Masses of the satellites of Uranus

S. F. Dermott & P. D. Nicholson

Center for Radiophysics and Space Research, Space Sciences Building, Cornell University, Ithaca, New York 14853, USA

The dynamical theory used to obtain the masses of the uranian satellites from their orbital precession rates contains a fundamental error. The masses can be derived from the precession rates, but a correct analysis of the available data must allow for the fact that the eccentricities, inclinations and precession rates all vary considerably with time, due to mutual secular perturbations.

THE Voyager 2 spacecraft should encounter Uranus on 24 January 1986 and we will then obtain the first detailed images of this puzzling and poorly understood system. Visual observations by Sir William Herschel in 1781 and Lassel in 1851 revealed the presence of four major satellites of similar size: Ariel, Umbriel, Titania and Oberon[1]. The comparatively small and innermost satellite, Miranda, was discovered photographically by Kuiper in 1948 (ref. 1). All of these satellites orbit the planet in direct, near-equatorial, near-circular orbits, but the dynamics of the system appear to be quite different from those of the satellite systems of Jupiter and Saturn. This difference has been insufficiently recognized, which has led to serious misinterpretations of the available observational information.

The radii and the masses of the satellites are presented in Table 1. Brown *et al.*[2] and Brown and Clark[3] determined the satellite radii from photometric and radiometric measurements using a version of the standard radiometric model developed for asteroids. The latest and most complete derivation of the satellites' orbital elements (Table 2) is due to Veillet[4], who has also determined the masses of the four larger satellites from the observed pericentre precession rates[5,6]. The striking feature of these results is the marked dichotomy in the derived satellite densities; the densities of Ariel and Umbriel are similar to those of the inner satellites of Saturn, and are consistent with a composition of 40% rock and 60% water-ice, but Titania and Oberon appear to have much higher densities, suggesting that the water-ice constitutes little more than a thin outer shell. Near-infrared reflectance spectra show that all five satellites have surfaces of water-ice contaminated with a dark spectrally neutral material showing spectral characteristics similar to those of, for example, carbonaceous chondritic material[7].

Table 1 Masses of the uranian satellites

j	Satellite	Radius* (km)	m/M† $\times 10^5$	m/M‡ $\times 10^5$	Densities§ (g cm^{-3})
1	Miranda	250±110	~0.1	0.2±0.2	—
2	Ariel	665±65	1.8±0.6	1.8±0.4	1.3±0.5
3	Umbriel	555±50	1.1±0.3	1.2±0.5	1.4±0.6
4	Titania	800±60	3.2±0.8	6.8±0.8	2.7±0.6
5	Oberon	815±70	3.4±1.0	6.9±0.8	2.6±0.6

* From ref. 2.

† Derived from the radii of Brown *et al.*[2] using a nominal density of 1.3 g cm^{-3}. The quoted uncertainties in the masses take no account of the uncertainties in the densities.

‡ From ref. 4.

§ Derived from the radii of Brown *et al.*[2] and the masses of Veillet.

A second unusual feature of the Uranus system is the fact that all five satellites have comparable non-zero orbital eccentricities. Since the prediction[8] and discovery[9] of active volcanism on Jupiter's satellite Io, it has been realized that tidal heating due to eccentricity damping may dominate the internal heat budgets of some satellites, so that the thermal evolution of some satellites cannot be understood without a concomitant understanding of their orbital evolution. This is certainly true for Io and may also be for Europa[10-12] and for the saturnian satellite Enceladus[13]. The observed orbital eccentricities and the calculated tidal damping timescales of the uranian satellites are shown in Table 2. It is puzzling that the inner satellites have tidal damping timescales much shorter than those of the outer satellites, probably much shorter than the age of the Solar System, even though all the orbital eccentricities are both finite and of similar magnitude[14,15].

We argue here that the problem posed by the satellite density distribution arises from a misunderstanding of the orbital